Locally Recurrent Central-Type Early Stage Lung Cancer < 1.0 cm in Diameter After Complete Remission by Photodynamic Therapy*

Kinya Furukawa, MD, PhD; Harubumi Kato, MD, PhD; Chimori Konaka, MD, PhD; Tetsuya Okunaka, MD, PhD; Jituo Usuda, MD, PhD; and Yoshiro Ebihara, MD, PhD

Background: **It is well known that central-type early stage lung cancer < 1.0 cm in diameter shows almost 100% complete response (CR) to photodynamic therapy (PDT). However, we have encountered cases of local recurrence after CR of tumors with a surface diameter < 1.0 cm.**
Patients and methods: **Ninety-three patients with 114 lesions were followed up, and cases of recurrence after CR has been obtained with initial tumors that had a diameter < 1.0 cm were examined. We compared the cytologic findings of local recurrence after CR to the cytologic findings before PDT. The relationship between the cell features and the depth of bronchial tumor invasion before PDT and on recurrence was evaluated.**
Results: **The CR and 5-year survival rates of patients with lesions < 1.0 cm were 92.8% (77 of 83 patients) and 57.9%, respectively; meanwhile, in the group of patients with lesions ≥ 1.0 cm, CR and 5-year survival rates were 58.1% (18 of 31 patients) and 59.3%. There was a significant difference in efficacy between the two groups ($p < 0.001$). Recurrences after CR were recognized in 9 of 77 lesions (11.7%) < 1.0 cm. When the recurrent tumor cells showed type I-II (low-to-moderate atypia) at the same site initially treated, CR could be obtained by a second PDT. Type III cells (high-grade atypia) showed the characteristics of tumor cells from deeper layers of the bronchial wall. Local recurrence at the same site may be caused by residual tumor cells from deep layers because of inadequate laser irradiation and penetration.**
Conclusions: **To reduce the recurrence rate, it is essential to accurately grasp the tumor extent and the depth of the bronchogenic carcinoma before performing PDT. Analysis of cell features of recurrent lesions after CR appears to be a useful source of information as to the depth of cancer invasion in the bronchial wall.** ***(CHEST 2005; 128:3269–3275)***

Key words: early stage lung cancer; occult lung cancer; photodynamic therapy; porfimer sodium

Abbreviations: AFB = autofluorescence bronchoscopy; CIS = carcinoma *in situ*; CR = complete remission; EBUS = endobronchial ultrasonography; ESLC = early stage lung cancer; PDT = photodynamic therapy; PR = partial remission

Lung cancer has a tendency to develop in older people, with a very poor prognosis. A total of 55,000 Japanese died from lung cancer in 2003, which made it the number-one cause of cancer death. Although diagnostic techniques such as high-resolution CT scan, video bronchoscopy, fluorescence bronchoscopy, and endobronchial ultrasonography (EBUS) have been developed recently, many patients with newly detected lung cancer still have inoperable advanced cancer. Therefore, the detection of early stage lung cancer (ESLC) is considered essential to reduce the mortality rate. Meanwhile, even when ESLC is detected, some cases are inoperable because of cardiopulmonary dysfunction due to age. Endoscopic procedures that are minimally invasive and do not compromise pulmonary function

*From the Department of Chest Surgery (Dr. Furukawa), Kasumigaura Hospital, Tokyo Medical University, Ibaraki; First Department of Surgery (Drs. Kato, Konaka, Usuda, and Ebihara), Second Department of Pathology, Tokyo Medical University, Tokyo; and Center for Respiratory Diseases (Dr. Okunaka), Sanno Hospital, Tokyo, Japan.
Manuscript received February 12, 2005; revision accepted May 9, 2005.

Correspondence to: Kinya Furukawa, MD, PhD, Department Chest Surgery, Tokyo Medical University, Kasumigaura Hospital, 3-20-1 Chuo, Ami-machi, Inashiki-gun, Ibaraki 300-0395, Japan; e-mail: k-furu@tokyo-med.ac.jp

are considered useful modalities for centrally located lung cancer. In particular, photodynamic therapy (PDT) is considered a useful and attractive modality for central-type ESLC.[1–7] Its action mechanism is considered to involve singlet oxygen, which is generated through photochemical reactions and causes degenerative necrosis of cells that have taken up the photosensitizer, *ie*, tumor cells.[8]

PDT using red laser light and a tumor-specific photosensitizer was established as a new therapeutic modality for central-type ESLC in 1982.[1] The length of longitudinal tumor extent was the only independent predictive factor for complete remission (CR), and 100% CR in lesions < 1.0 cm in diameter treated by PDT was reported.[5] However, we have encountered local recurrences after CR of tumor even in cases with a surface diameter < 1.0 cm. Therefore, we investigated the characteristics and cytomorphologic features of primary lesions and recurrences after CR in patients with lesions < 1.0 cm in diameter.

Materials and Methods

Patient Selection

A total number of 145 patients with 191 lesions of endoscopic ESLC underwent PDT from February 1980 to April 2001 in the Department of Tokyo Medical University. Of the 145 patients with 191 lesions, 93 patients with 114 lesions were followed up, and cases of recurrence after CR was obtained with initial tumors with a diameter < 1.0 cm were examined.

Procedures of PDT and Follow-up

The depth of tumor invasion was judged by biopsy specimen and CT scan, and was also evaluated by bronchoscopic findings based on the diagnostic criteria of ESLC defined by the Japan Lung Cancer Society.[9] To determine tumor size, bronchoscopic biopsies of the proximal and distal sites of the lesion and bronchoscopic measurements using forceps were performed. PDT procedures were performed with the combination of porfimer sodium (Photofrin; Wyeth Japan K.K.; Tokyo, Japan) that is taken up selectively in tumor, and an argon gas laser system (model 770; Spectra-Physics; Mountain View, CA) or excimer dye laser (EDL-1; Hamamatsu Photonics; Hamamatsu, Japan). Laser irradiation was performed via a quartz fiber inserted through the biopsy channel of the endoscope at 48 h after the IV administration of 2.0 mg/kg of porfimer sodium. The total energy of the laser irradiation was 100 J/cm^2, and energy levels in this range do not cause any heat degeneration or other adverse effects. The duration of irradiation required usually 10 to 20 min. Clean-up bronchoscopies to remove necrotic tissue produced by the PDT reaction were performed at 1, 3, and 7 days after PDT. Both cytologic and histologic examinations via fiberoptic bronchoscopy were performed at 1, 2, and 3 months, and thereafter at 3-month intervals in the first year and 6-month intervals after the second year until 5 years after PDT.

Efficacy Evaluation

The antitumor effect of initial treatment was rated based on endoscopic measurement of tumor size using forceps, morphologic observations, and histopathologic examination by biopsy, according to the general rules of the Japan Lung Cancer Society[9] and the Japan Society of Clinical Oncology.[10] The antitumor effect was rated at 1 month and 2 months after PDT. Antitumor effect was rated as CR (no demonstrable tumor microscopically by brushing and/or biopsy for a period of 4 weeks), partial remission (PR) [$\geq 50\%$ reduction in tumor size], no change ($< 50\%$ reduction or $< 25\%$ increase in tumor size), progressive disease ($> 25\%$ increase in tumor size), or not evaluable.

Evaluation of Cytomorphologic Features of Local Recurrences

In the central-type ESLC < 1.0 cm in greatest dimension, we have compared the cytologic findings of local recurrence after CR to the cytologic findings before PDT using bronchial brushing specimen. Cytologic findings were classified into three cytologic morphotypes using the classification of cell features proposed by Konaka and coworkers,[11] which appears to yield information as to the depth of cancer invasion in the bronchial wall. The classification was described as follows: type I cell, low-grade atypia (resembling atypical squamous cell metaplasia); type II cell, moderate-grade atypia (resembling early stage squamous cell carcinoma); and type III cell, high-grade atypia (resembling invasive squamous cell carcinoma). The biopsy specimens before PDT and on recurrence, or resected materials, in cases of resection after recurrence, were examined histopathologically, and the depth of bronchial wall invasion was classified into three groups: grade 1, carcinoma *in situ* (CIS) or microinvasion; grade 2, extramuscular bronchial wall invasion; and grade 3, intracartilaginous to extracartilaginous invasion. The relationship between the cell features and the depth of bronchial tumor invasion before and after PDT was evaluated.

Statistical Analysis

Statistical analysis were done using statistical software (Stat Flex for Windows, version 5.0; Artec; Osaka, Japan). The χ^2 test was used to compare the efficacy of PDT between lesions < 1.0 cm and > 1.0 cm in diameter. Differences between the survival rates of two groups in the Kaplan-Meier survival curves were analyzed using the log-rank test; $p < 0.05$ was considered to indicate a statistically significant difference.

Results

Results of PDT for Central-Type ESLC

A total of 93 patients with 114 lesions of central-type ESLC who underwent PDT were examined. Thirteen synchronous lesions in six cases, 15 metachronous lesions in six cases, and 5 synchronous/metachronous lesions in one case were observed. The evaluation of the efficacy of PDT is shown in Table 1. CRs and PRs were obtained in 75 patients with 95 lesions (83.3%) and in 18 patients with 19 lesions (16.7%) out of 93 patients with 114 lesions. Each lesion with PR was subsequently treated with other modalities, including surgery in 13 cases, chemotherapy in 5 cases, or radiotherapy in 1 case, and finally achieved 100% CR. Recurrences after CR were recognized in 12 of 95 lesions (12.6%). The 114 lesions were classified in two groups according to the

Table 1—*Results of PDT for Central-Type ESLC

Tumor Size, cm	Lesions, No.	CR	PR	Recurrence After CRT
< 1.0	83	77 (92.8)	6 (7.2)	9 (11.7)
≥ 1.0	31	18 (58.1)	13 (41.9)	3 (16.7)
Total	114	95 (83.3)	19 (16.7)	12 (12.6)

*Data are presented as No. (%) unless otherwise indicated.
†p < 0.001.

maximum longitudinal tumor extent. Of these, 83 lesions (72.8%) were < 1.0 cm and 31 lesions (27.2%) were ≥ 1.0 cm in diameter. The CR and PR rates in the group of patients with lesions < 1.0 cm in maximum diameter were 92.8% (77 of 83 patients) and 7.2% (6 of 83 patients), respectively. Meanwhile, in the group of patients with lesions ≥ 1.0 cm in diameter, the CR and PR rates were 58.1% (18 of 31 patients) and 41.9% (13 of 31 patients), respectively. Neither no change nor partial disease were observed in these groups. There was a significant difference in efficacy between the two groups using the χ^2 test ($p < 0.001$). Recurrences after CR were recognized in 9 of 77 lesions (11.7%) in the group < 1.0 cm and 3 of 18 lesions (16.7%) in the group ≥ 1.0 cm in diameter. The overall 5-year survival rates of the two groups were 57.9% and 59.3%, respectively (Fig. 1). There was no significant difference between the two groups on the basis of the log-rank test ($p = 0.207$).

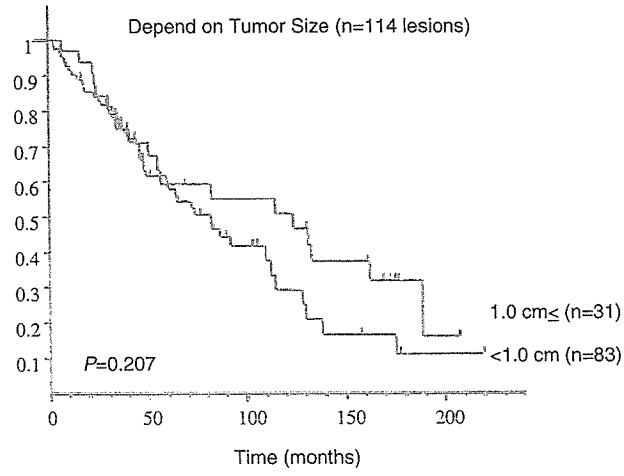

FIGURE 1. The overall 5-year survival rates were 57.9% in the group of patients with tumors < 1.0 cm and 59.3% in the group with tumors ≥ 1.0 cm in diameter, respectively. There was no significant difference between the survival rates of two groups in the Kaplan-Meier curves on the basis of the log-rank test ($p = 0.207$).

Characteristics of Local Recurrence < 1.0 cm in Diameter After CR

The information on nine patients with nine lesions in the group of patients with lesions < 1.0 cm in diameter who had recurrence after CR had been achieved by initial PDT are presented in Table 2. All patients with recurrence were male, and the age distribution ranged from 64 to 71 years (average age, 67.6 years at the time of initial diagnosis). Evidences of local recurrence were found in nine patients with nine lesions at the site of the primary lesion. The recurrent lesions were located on the trachea in one patient, lobar bronchus in one patient, segmental bronchi in five patients, and subsegmental bronchi in two patients. The average diameter of the nine recurrent lesions was 0.46 cm. All lesions were squamous cell carcinoma, and endoscopic findings showed nodular type in two lesions and superficial type in seven lesions. The disease-free interval of these nine patients ranged from 3 to 18 months (average, 10 months).

Local recurrence at site corresponding to the

Table 2—*Recurrent Cases After PDT for Central-Type ESLC < 1.0 cm in Diameter*

Case No.	Patient Age, yr	Lesion	Size, cm	BF Findings	CR, mo	Recurrence	Additional Treatment	Prognosis
1	66	Segmental bronchus rB^3	0.3	Superficial	18	PM	PDT, OP (RUL)	Alive (24 mo)
2	64	Subsegmental bronchus IB^3 a-b	0.3	Superficial	13	PM	PDT, OP (LPn)	Dead (56 mo), other disease
3	69	Subsegmental rB^{10} a-b	0.4	Superficial	10	PM	PDT Brachy	Alive (41 mo)
4	64	Segmental bronchus IB^{1+2}	0.6	Nodular	5	SS (CIS)	PDT	Alive (24 mo)
5	66	Segmental bronchus rB^1	0.5	Superficial	3	SS (CIS)		Dead (5 mo), other disease
6	69	Segmental bronchus IB^{1+2}	0.4	Superficial	14	SS (CIS)	PDT	Alive (27 mo)
7	71	Trachea	0.3	Nodular	10	SS (CIS)	PDT	Alive (27 mo)
8	70	Lobar bronchus rMid.-low	0.9	Superficial	6	SS (intracartilage)	OP (RML)	Dead (56 mo), other disease
9	69	Segmental IB^{1+2} B^3	0.4	Superficial	11	SS (extracartilage)	Nd-YAG, radiation, OP	Alive (65 mo)

*PM = peripheral margin initially treated; SS = same site initially treated; OP = operation; RML = right middle lobe; RUL = right upper lobe; LPn = left pneumonectomy; BF = bronchofiberscopic.

Table 3—*Cell Feature and Depth of Bronchial Invasion*

Case No.	Before PDT		Recurrence	
	Cytology (Brush) Type	Pathologic Grade	Cytology (Brush) Type	Pathologic Grade
4	I	1	I	1
5	I	1	I	1
6	I–II	1	I–II	1
7	I	1	II	1
8	I–II	1	II–III	3 (intracartilaginous invasion)
9	I	1	III	3 (extracartilaginous invasion)

peripheral margin of the lesion initially treated by PDT was observed in three patients (cases 1 to 3), while local recurrence at the same site as the initial tumor initially treated was observed in six patients (cases 4 to 9). The local recurrences at the site corresponding to the peripheral lesion were initially located in the subsegmental bronchus in two of three primary lesions. The patients with three local recurrences at the site corresponding to the peripheral margin underwent a second PDT session; however, CR was not obtained in any of these patients. Therefore, additional conventional surgery was performed in two patients and brachytherapy in one patient. The pathologic examinations of two operated patients showed residual tumor at the peripheral site. Right upper lobectomy was performed for case 1, and the resected material revealed superficial tumor invasion peripheral to the right B^3b. Left pneumonectomy was selected for case 2 (ipsilateral double cancer) because an ESLC was located at the bifurcation of left B^3a-b and a malignant lymphoma was in left B^6. This patient died due to malignant lymphoma at 56 months after the initial PDT session. Four patients (cases 4 to 7) with six local recurrences at the same site as the initial tumor local showed superficial tumor invasion (CIS), and a second PDT session was performed in three of four patients. CRs were again obtained in all three patients, who are presently disease free. One double cancer patient who had advanced stomach cancer underwent systemic chemotherapy without a second PDT but died 5 months after the initial PDT session. The pathologic examinations of the two other surgically treated patients (cases 8 and 9) revealed intracartilagious invasion of the bronchial wall. One multiple lung cancer patient (case 8) who received right middle and lower lobectomy after local recurrence died of hemoptysis due to another advanced lung cancer at 56 months after the initial PDT session. At the last follow-up of the nine patients who had local recurrence after CR had been obtained by initial PDT in whom the original primary lesion had been < 1.0 cm

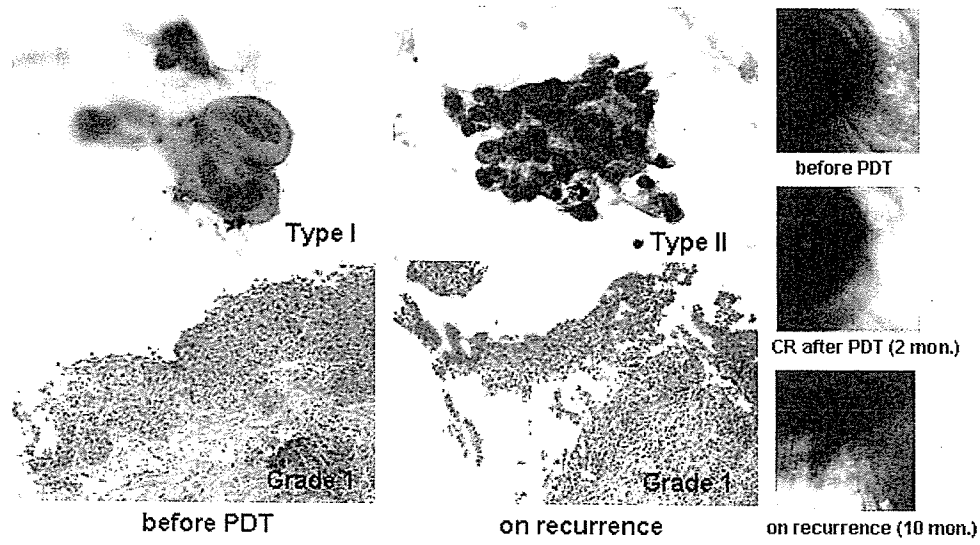

FIGURE 2. The cytopathologic and bronchoscopic findings in case 7. Bronchoscopic findings showed a small nodular tumor at the right side of the tracheal wall before PDT. Redness of the tracheal mucosa was observed on recurrence at 10 months after PDT. Cytologic findings before PDT were classified as type I because cell features showed a round shape and slight increase of nuclear chromatin but low-grade nuclear atypia. The biopsy specimen showed CIS (grade 1). Cytologic findings on recurrence were classified as type II because a sheet formation of polymorphic-shaped cells, increase of nuclear chromatin, and nuclear body were observed. Biopsy specimen on recurrence showed superficial tumor invasion (CIS) beneath the thin epithelial layer (grade 1). A second PDT was performed, and CR was again obtained in this patient.

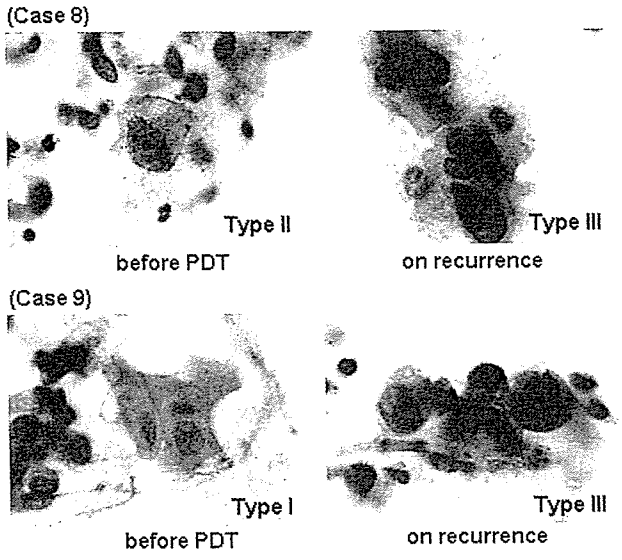

FIGURE 3. The findings of brushing cytology mainly observed in cases 8 and 9 before PDT and on recurrence after CR. Cytologic findings before PDT in case 8 were classified as type II because of a slight increase of nuclear chromatin. Cytologic findings before PDT in case 9 were classified as type I because of low-grade nuclear atypia. The findings of recurrent tumor cells in cases 8 and 9 were classified as type III because of severe increases of nuclear chromatin, high nuclear/cytoplasmic ratio, and high grade of nuclear atypia.

in diameter, three patients had died of other diseases and six patients were alive, and there were no deaths from the primary lesion.

Evaluation of Cytomorphologic Features of Local Recurrences

As mentioned above, local recurrence of the carcinoma at the same site as lesions < 1.0 cm in diameter initially treated successfully by PDT was observed in six out of nine locally recurrent patients (cases 4 to 9). A summary of the cell features and depth of bronchial wall invasion before PDT and after recurrence are shown in Table 3. The brushing cytology specimens before PDT mainly showed type I or II, and biopsy revealed grade 1 in all six cases. The majority of cell features in cases 4 to 7 showed type I or II, and the biopsy specimens showed grade 1 on recurrences. The cytopathologic and bronchoscopic findings of case 7 are shown Figure 2. Populations of type I and II cells were predominant in the recurrent lesions in these cases, which implied that the recurrent tumor was located in a superficial layer of bronchial wall. When the recurrent tumor cells showed type I-II (low-to-moderate atypia) local recurrence at the same site as the initial tumor initially treated, CR could be obtained by a second PDT. In cases 8 and 9, mainly type III cell features were observed in brushing cytology on recurrence (Fig 3). These two cases underwent resection, and the resected specimens revealed intracartilaginous tumor invasion of bronchial wall (grade 3), which implied the residual tumor located in a deep layer of bronchial wall.

DISCUSSION

PDT for cancer using a combination of low-power laser irradiation and tumor specific photosensitizer was first applied clinically by Dougherty et al[12] in 1978 to the skin metastasis of breast cancer. Since then, we performed the first reported endoscopic clinical application of PDT in cooperation with Dougherty and coworkers.[12] In Japan, PDT using porfimer sodium, a tumor-specific photosensitizer and excimer dye laser, was recognized by the government; and from April 1996, hospitals could receive reimbursement for PDT of early stage carcinomas of the lung, esophagus, stomach, and cervix from the national health insurance system.

The best PDT candidates in lung cancer are cases with central-type ESLC because of their endoscopic accessibility; therefore, selection of patient is important to achieve CR. Nagamoto et al[13] demonstrated that no lymph node involvement was found in 59 cancers with a longitudinal extent of < 20 mm; in another study,[14] histology by serial block sectioning showed that there was no nodal involvement in any CIS cases. Nakamura et al[15] retrospectively analyzed resected cases of central-type ESLC to clarify the relation between the endoscopic findings and the histologic extent of tumor. They demonstrated a significant difference is the maximum dimension according to the depth of bronchial invasion between CIS and extramuscular invasion and CIS and invasion into or beyond the cartilaginous layer. Lesions with a maximum diameter < 1.0 cm have a high possibility of being CIS. Their preoperative bronchoscopic diagnosis of centrally located ESLC was correct in 74.0%. In another study, Akaogi et al[16] demonstrated that polypoid or nodular lesions < 1.0 cm and flatly spreading lesions < 1.5 cm in greatest dimension were limited to within the cartilaginous layer without regional lymph node involvement. Also, Furuse et al[5] demonstrated that the length of longitudinal tumor extent was the only independent predictive factor for CR by PDT, and that lesions < 1.0 cm in diameter showed 100% CR. According to these data, therapy for CR requires satisfaction of the following endoscopic conditions: (1) no evidence of lymph node metastasis; (2) the lesion is superficial with a maximum diameter of < 1.0 cm; (3) no invasion into or beyond the cartilaginous layer; (4) the histologic type is squamous cell carcinoma; and

(5) the lesion is located in a position that can be easily irradiated with the laser.

In this study, excellent efficacy with a significant difference of CR rate was seen in patients with lesions < 1.0 cm (92.8%) compared to ≥ 1.0 cm (58.1%) in diameter; however, the overall 5-year survival rate of the two groups showed no significant difference (57.9% vs 59.3%). This may be because it was possible to perform additional alternative modalities such as surgery, second PDT, and brachytherapy to achieve CR after failure of initial PDT or recurrence after PDT. Considering that the 5-year survival rate of pathologic stage Ia (T1N0M0) patients who underwent surgery is approximately 67.0%,[17] our data are favorable because the majority of the PDT group consisted of patients with advanced age and poor cardiopulmonary function. Therefore, we consider that PDT may be used as first-line therapy for central-type ESLC prior to surgery, especially in cases with poor cardiopulmonary function. Also, Edell et al[18] and Cortese et al[19] demonstrated that PDT is an alternative to surgical resection in the management of early superficial squamous cell carcinoma.

In this study, recurrence after CR was recognized in 9 of 77 lesions (11.7%) in the group of patients with lesions < 1.0 cm in diameter. Despite the average diameter of the nine initial lesions being relatively small (0.46 cm), recurrence was recognized in eight of nine lesions (88.9%) within 12 months. Therefore, intensive follow-up studies should be performed until 1 year after PDT even for small primary lesions. The reasons why recurrences after CR were observed in the lesions < 1.0 cm in diameter could be explained by inappropriate estimation of the peripheral margin in cases of local recurrence at the site corresponding to the peripheral margin and insufficient laser irradiation or miss estimation of tumor depth in the cases of local recurrence at the same site as the initial tumor.

From our experiences, to achieve CR with PDT for central-type ESLC, it appears that not only the analysis of cell features but also the comprehension of tumor extent to the peripheral site and tumor invasion to the bronchial wall are of considerable significance. Kurimoto et al[20] demonstrated that endobronchial EBUS was useful to determine the depth of tumor invasion into the bronchial wall, and the accuracy of EBUS from the histopathologic findings was 95.8%. The EBUS image at 20 MHz shows five layers in the cartilaginous portion of bronchial wall. The third to fifth layers are images of cartilage. Therefore, it is feasible to evaluate the depth of invasion using EBUS whether or not the tumor invades into or beyond the cartilaginous layer.. In lesions with an intact third layer on EBUS, CR could be achieved with PDT. Miyazu et al[21] demonstrated that the depth of tumor invasion estimated by EBUS was accurate by histopathologic findings after surgical resection. They found 5 of 14 lesions (35.7%) < 1.0 cm in diameter that showed extracartilaginous invasion on the EBUS image that was later confirmed histopathologically; also, 3 of 5 lesions appeared bronchoscopically superficial but were shown to be extracartilaginous by EBUS. The indications of PDT for centrally located ESLC with a longitudinal extension of < 1.0 cm are unquestionable; meanwhile, we should realize that even < 1.0 cm in diameter can have extracartilaginous invasion. To comprehend the surface extent of superficial tumor invasion in the bronchial lumen, autofluorescence bronchoscopy (AFB) is considered useful.[22–25] The green autofluorescence of the lesion was decreased because of the lack of endogenous fluorophors, thickening of the membrane, and increased microvasculature.[26] We sometimes encountered unexpected surface invasion by AFB.

It is essential to know the extent of the tumor and the depth of bronchogenic carcinoma accurately for the selection of treatment modality. Corresponding to the previous study by Konaka et al,[11] the analysis of cell features is a useful source of information to evaluate the depth of cancer invasion in the bronchial wall. In addition, we believe that it could be beneficial information when choosing the treatment modality, such as recurrence after CR by PDT demonstrated in our study. Additionally, we now perform EBUS and AFB to determine the indications of PDT in all patients who have ESLC for the purpose of achieving 100% CR and reduction of recurrence rate. A comparative study of PDT for the treatment of ESLC before and after the adoption of EBUS and AFB will enable accurate evaluation of the benefits of these new diagnostic tools in the near future.

ACKNOWLEDGMENT: The authors are indebted to Professor J. P. Barron of the International Medical Communications Center of Tokyo Medical University for his review of this article.

REFERENCES

1 Hayata Y, Kato H, Konaka C, et al. Hematoporphyrin derivative and laser photoradiation in the treatment of lung cancer. Chest 1982; 81:269–277

2 Kato H, Konaka C, Kawate N, et al. Five-year disease-free survival of a lung cancer patient treated only by photodynamic therapy. Chest 1986; 90:768–770

3 Edell ES, Cortese DA. Bronchoscopic phototherapy with hematoporphyrin derivative for treatment of localized bronchogenic carcinoma: a 5-year experience. Mayo Clin Proc 1987; 62:8–14

4 Edell ES, Cortese DA. Bronchoscopic localization and treatment of occult lung cancer. Chest 1989; 96:919–921

5 Furuse K, Fukuoka M, Kato H, et al. A prospective phase II

study on photodynamic therapy with Photofrin II for centrally located early-stage lung cancer. J Clin Oncol 1993; 11:1852–1187
6 Kato H. Photodynamic therapy for lung cancer: a review of 19 years' experience. J Photochem Photobiol 1998; B42:96–99
7 Kato H, Furukawa K, Sato M, et al. Phase II clinical study of photodynamic therapy using mono-L-aspartyl chlorin e6 and diode laser for early superficial squamous cell carcinoma of the lung. Lung Cancer 2003; 42:103–111
8 Niedre M, Patterson MS, Wilson BC. Direct near-infrared luminescence detection of singlet oxygen generated by photodynamic therapy in cells *in vitro* and tissues *in vivo*. Photochem Photobiol 2002; 75:382–391
9 General rules for clinical and pathological records of lung cancer. 4th ed. In: Japan Lung Cancer Society, eds. Tokyo, Japan: Kanehara and Company, 1995; 123–133
10 Niiya H. Toxicity grading criteria of the Japan Clinical Oncology Group. Int J Clin Oncol 1997; 32:61–65
11 Konaka C, Miura H, Ikeda N, et al. The characteristics of early bronchogenic carcinoma evaluated by cytomorphological features. Lung Cancer 2002; 38:267–271
12 Dougherty TJ, Lawrence G, Kaufman JH, et al. Photoradiation in the treatment of recurrent breast carcinoma. J Natl Cancer Inst 1978; 62:231–237
13 Nagamoto N, Saito Y, Ohta S, et al. Relationship of lymph node metastasis to primary tumor size and microscopic appearance of roentgenographically occult lung cancer. Am J Surg Pathol 1989; 13:1009–1013
14 Nagamoto N, Saito Y, Sato M, et al. Clinicopathological analysis of 19 cases of isolated carcinoma in situ of the bronchus. Am J Surg Pathol 1993; 17:1234–1243
15 Nakamura H, Kawasaki N, Hagiwara M, et al. Endoscopic evaluation of centrally located early squamous cell carcinoma of the lung. Cancer 2001; 91:1142–1147
16 Akaogi E, Ogawa I, Mitsui K, et al. Endoscopic criteria of early squamous cell carcinoma of the bronchus. Cancer 1994; 74:3113–3117
17 Mountain CF. Revisions in the international system for staging lung cancer. Chest 1997; 111:1710–1717
18 Edell ES, Cortese DA. Photodynamic therapy in the management of early superficial squamous cell carcinoma as an alternative to surgical resection. Chest 1992; 102:1319–1322
19 Cortese DA, Edell ES, Kinsey JH. Photodynamic therapy for early stage squamous cell carcinoma of the lung. Mayo Clin Proc 1997; 72:595–602
20 Kurimoto N, Murayama M, Yoshioka S, et al. Assessment of usefulness of endobronchial ultrasonography in determination of depth of tracheobronchial tumor invasion. Chest 1999; 115:1500–1506
21 Miyazu Y, Miyazawa T, Kurimoto N, et al. Endobronchial ultrasonography in the assessment of centrally located early-stage lung cancer before photodynamic therapy. Am J Respir Crit Care Med 2002; 165:832–837
22 Lam S, Kennedy T, Unger M, et al. Localization of bronchial intraepithelial neoplastic lesions by fluorescence bronchoscopy. Chest 1998; 113:696–702
23 Ikeda N, Hiyoshi T, Kakihana M, et al. Histopathological evaluation of fluorescence bronchoscopy using resected lungs in cases of lung cancer. Lung Cancer 2003; 41:303–309
24 Sutedja TG, Codrington H, Risse EK, et al. Autofluorescence bronchoscopy improves staging of radiographically occult lung cancer and has an impact on therapeutic strategy. Chest 2001; 120:1327–1332
25 Sutedja TG, Venmans BJ, Smit EF, et al. Fluorescence bronchoscopy for early detection of lung cancer: a clinical perspective. Lung Cancer 2001; 34:157–168
26 Furukawa K, Ikeda N, Miura T, et al. Is autofluorescence bronchoscopy needed to diagnose early bronchogenic carcinoma? J Bronchol 2003; 10:64–69

CHEST®

Official publication of the American College of Chest Physicians

Quantitative Detection of Lung Cancer Cells by Fluorescence In Situ Hybridization: Comparison With Conventional Cytology

Haruhiko Nakamura, Idiris Aute, Norihito Kawasaki, Masahiko Taguchi, Tatsuo Ohira and Harubumi Kato

Chest 2005;128;906-911
DOI 10.1378/chest.128.2.906

Quantitative Detection of Lung Cancer Cells by Fluorescence *In Situ* Hybridization*

Comparison With Conventional Cytology

Haruhiko Nakamura, MD, PhD; Idiris Aute, MD, PhD; Norihito Kawasaki, MD; Masahiko Taguchi, MD, PhD; Tatsuo Ohira, MD, PhD; and Harubumi Kato, MD, PhD, FCCP

Study objective: **The aim of this study was to clarify whether fluorescence *in situ* hybridization (FISH) can diagnose lung cancer in various clinical specimens in comparison with conventional cytology.**
Design: **Prospective study.**
Setting: **University hospital in a metropolitan area.**
Patients: **Fifty consecutive patients with abnormal chest radiography or CT scan findings were enrolled. The patients included 32 men and 18 women, with an average age of 64 years. The final definitive diagnosis was made by histologic examination, as follows: 38 primary lung cancers (24 adenocarcinomas, 8 squamous cell carcinomas, 2 large cell carcinomas, and 4 small cell carcinomas); 1 metastatic renal cell carcinoma; and 11 benign lesions.**
Methods: **Four types of clinical specimens were analyzed. Cells obtained by transbronchial brushing and transbronchial fine-needle aspiration using a fiberoptic bronchoscope under fluoroscopy, CT scan-guided percutaneous needle biopsy, and bronchial washings. On every examination, duplicate slides were made for analyses of conventional cytology and FISH.**
Results: **Classifications according to conventional cytology were as follows: class I, 4 patients; class II, 15 patients; class IIIa, 3 patients; class IIIb, 5 patients; and class V, 23 patients. A classification higher than class IIIb was considered to be positive for cancer. For cytology, we found no false-positive cases and 11 false-negative cases. The specificity was 100%, and the sensitivity was 71.8%. By FISH, 34 cases showed aberrant copy numbers in either chromosome 3 or 17. We found no false-positive cases and five false-negative cases. The specificity was 100%, and the sensitivity was 87.1%.**
Conclusion: **The ability of FISH to detect aneusomic lung cancer cells is superior to conventional cytology for the diagnosis of lung cancer.** ***(CHEST 2005; 128:906–911)***

Key words: aneuploidy; aneusomy; cytology; fluorescence *in situ* hybridization; lung cancer

Abbreviations: BW = bronchial washing; FISH = fluorescence *in situ* hybridization; PN = percutaneous needle biopsy; SSC = standard saline citrate; TB = transbronchial brushing

Conventional cytology plays an important role for the diagnosis of lung cancer, especially in the examination of sputum and pleural effusions. In addition, cell specimens obtained by transbronchial brushing (TB)[1] and needle aspiration under fluoroscopy,[2] percutaneous needle biopsy (PN) under CT scanning,[3] and bronchial washings (BWs)[4] provide important information for the differential diagnosis between benign and malignant disease. Cytologic diagnoses are made by experienced cytologists who can properly evaluate the morphologic features of malignant cells. However, this judgment is some-

*From the Department of Chest Surgery (Drs. Nakamura, Kawasaki, and Taguchi), Atami Hospital, International University of Health and Welfare, Atami, Shizuoka, Japan; the Department of Thoracic Surgery (Dr. Aute), The First Affiliated Hospital, Xinjiang Medical University, Urumqi, People's Republic of China; and the Department of Surgery (Drs. Ohira and Kato), Tokyo Medical University, Tokyo Japan.
Supported by grant No. 15591493 from the Ministry of Education, Science, Sports, and Culture in Japan.

Manuscript received September 2, 2004; revision accepted January 13, 2005.

Correspondence to: Haruhiko Nakamura, MD, PhD, Department of Chest Surgery, Atami Hospital, International University of Health and Welfare, 13-1 Higashikaigan-cho, Atami-city, Shizuoka, Japan 413-0012; e-mail: h.nakamura@iuhw.ac.jp

times difficult when the morphologic changes associated with malignancy are mild. Such cells are usually classified as class III, using the classification of Papanicolaou,[5] which is suggestive of, but not conclusive for, malignancy. This is an ambiguous judgment for clinical decision making. In addition, when one obtains a small number of cells from the lesion, the definitive diagnosis is even more difficult. These limitations of morphology-based conventional cytology have stimulated the search for more objective and quantitative methods for an accurate cytologic diagnosis of cancer.

Aneuploidy is the most common feature of many solid tumors, including lung cancer.[6] Solid tumors are characterized by complicated karyotypes by classic cytogenetics.[7,8] Chromosomal instability[9,10] may cause the uneven distribution of chromosomes during cell division.[11,12] Thus, malignant tumors can be diagnosed by detecting aneuploid, usually hyperdiploid, cells. A rapid and sensitive method for detecting aneusomy of a specific chromosome in an individual cell is fluorescence *in situ* hybridization (FISH). For this purpose, specific centromeric DNA probes enumerated the chromosomes. FISH was originally developed as a method to detect chromosomal aberrations,[13] and is now widely used for gene mapping,[14] the diagnosis of congenital diseases,[15] and detecting specific gene copy number changes in malignant cells.[16–18]

One advantage of FISH in detecting malignant cells is its objective and quantitative evaluation. However, the specificity and sensitivity of FISH in the diagnosis of lung cancer is unclear. We report the results of a prospective study comparing FISH with conventional cytology to detect lung cancer cells.

Materials and Methods

Patients

Fifty consecutive patients who underwent cytologic examination for abnormal chest radiography or CT scan findings at Tokyo Medical University Hospital from July 2003 to January 2004 were enrolled in this prospective study. The patients included 32 men and 18 women, with an average age of 64 years. The final definitive diagnosis was made by histologic examination, as follows: 38 primary lung cancers (24 adenocarcinomas, 8 squamous cell carcinomas, 2 large cell carcinomas, and 4 small cell carcinomas); 1 metastatic renal cell carcinoma; and 11 benign lesions. All patients with lung cancer were staged according to the latest Union Internationale Centre le Cancer criteria.[19] Cases included 10 tumors in stage IA, 5 in stage IB, 1 in stage IIA, 3 in stage IIB, 10 in stage IIIA, 6 in stage IIIB, and 3 in stage IV (Table 1).

Cells gathered from lung lesions were independently analyzed by conventional cytology and FISH. Informed consent for the cytologic examinations and genetic analyses of the specimens were obtained from all patients.

Table 1—*Histology and Stage of Lung Cancer in This Series of Patients

Case	Age	Gender	Specimen	Histology	Stage
1	59	M	TB	Sq	cIIIA
2	42	F	PN	B	NA
3	43	M	TB	Ad	PIIIA
4	70	M	TB	Ad	CIV
5	77	M	TB	Ad	PIA
6	73	M	PN	Ad	PIA
7	58	M	TN	Ad	PIA
8	71	M	BW	Ad	pIIIA
9	71	M	BW	La	pIB
10	66	F	TN	RCC	NA
11	65	F	TB	Sm	cIIIB
12	68	F	PN	Ad	pIA
13	69	F	BW	Ad	pIV
14	52	F	TB	Ad	pIIA
15	75	F	TN	Sq	pIA
16	37	M	PN	B	NA
17	64	M	PN	Ad	pIIB
18	58	F	TB	B	NA
19	73	F	PN	Ad	pIA
20	62	M	PN	B	NA
21	69	M	TB	B	NA
22	76	M	BW	La	cIIIB
23	76	M	PN	Ad	cIIIB
24	75	M	PN	Ad	pIB
25	65	M	BW	Sm	cIIIA
26	23	M	PN	B	NA
27	74	M	BW	Ad	cIV
28	72	F	PN	B	NA
29	80	M	TB	B	NA
30	56	M	BW	Ad	pIB
31	64	M	TB	B	NA
32	58	M	PN	Ad	cIIIA
33	72	F	PN	Ad	pIA
34	72	M	PN	Ad	cIIIA
35	66	F	TB	Sm	cIIIB
36	61	M	TB	Ad	pIIB
37	72	F	TB	Ad	pIB
38	52	M	PN	B	NA
39	64	M	TB	Ad	pIA
40	79	F	TB	Sq	cIB
41	39	M	TB	B	NA
42	78	M	BW	Sq	cIIIB
43	62	M	TB	Sq	cIIIA
44	57	M	TB	Sq	pIIIA
45	70	M	PN	Ad	pIA
46	55	F	PN	Ad	pIA
47	58	F	TN	Sq	cIIIB
48	66	F	TN	Ad	pIIB
49	62	M	BW	Sm	cIIIA
50	72	F	BW	Sq	cIIIA

*M = male; F = female; TN = transbronchial needle biopsy; Ad = adenocarcinoma; Sq = squamous cell carcinoma; La = large cell carcinoma; Sm = small cell carcinoma; RCC = renal cell carcinoma; B = benign lesion; c = clinical stage; p = pathologic stage; NA = not applicable.

Cell Samples

In this study, the following four types of cell specimens were analyzed: cells obtained by TB (n = 18) and transbronchial fine-needle aspiration (n = 5) using a fiberoptic bronchoscope

under fluoroscopy, CT scan-guided PN using the 19-gauge Tokyo Medical University Needle[3] (n = 17), and BWs (n = 10). On every examination, duplicate specimens were made for simultaneous analyses of conventional cytology and FISH.

For conventional cytology, cells were stained by the Papanicolaou method. [5] Diagnosis was made by cytologists in the Department of Pathology at Tokyo Medical University Hospital. The various classes in conventional cytology are defined as follows: class I, absence of atypical or abnormal cells; class II, atypical cytology but no evidence of malignancy; class III, cytology suggestive of, but not conclusive for, malignancy (IIIa, mild dysplasia; IIIb, advanced dysplasia); class IV, cytology strongly suggestive of malignancy; and class V, cytology conclusive for malignancy.[5]

FISH

For FISH, cells on glass slides were air-dried overnight and stored at −80°C until they were used. Direct fluorochrome-labeled centromeric probes were used for the enumeration of different chromosomes. Spectrum-orange-labeled or Spectrum-green-labeled probes for the respective centromeric regions of chromosomes 3 and 17 were purchased (Vysis Inc; Downers Grove, IL), and dual-color FISH was performed. Slides were denatured by incubation with 70% formamide (two times the standard saline citrate [SSC] solution) at 74°C for 2 min in a water bath. Then, slides were dehydrated through a graded ethanol system (70% for 2 min, 85% for 2 min, and 100% for 2 min). A hybridization solution (10 μL) was applied to each slide, which was coverslipped and sealed with rubber cement. The hybridization solution contained 1 μL each DNA probe in 70% formamide (two times the SSC solution), and 10% dextran sulfate solution (cot I DNA). After incubation for 16 h at 37°C in a humidified chamber, slides were washed (two times SSC solution) for 3 min at 74°C. A di-amidinophenylindole antifade solution (8 μL) was applied to each spot and coverslipped. The slides were observed under a fluorescence microscope that was connected to a cooled charge-coupled device camera and an image analyzer system (CytoVision; Applied Imaging, Ltd; Newcastle, UK).

FISH signal analysis was performed as follows. All cells in a fluorescence microscopy field, except for those with damaged or overlapped nuclei, were evaluated. One hundred cells were counted, and the numbers of each centromeric signal were recorded. If there were < 100 cells on the slide, as many cells as possible were counted. When the percentages of hyperdisomic cells (*ie*, more than three copies for at least one chromosome) were > 10%, we judged the lesion to be malignant.

Comparison of Conventional Cytology and FISH

FISH diagnoses were made without clinical information or the results of conventional cytology. The results of FISH analysis were not shown to the cytologists. Thus, both diagnoses were independently made in a blind fashion.

Statistical Analysis

Differences in the number of countable cells according to the histology of the lung lesions or the cell-gathering methods used were analyzed by the Kruskal-Wallis test. A p value of < 0.05 was considered to be significant.

Results

Cells countable for FISH analyses ranged from 5 to 100 (maximum). Cell counts according to the cell-gathering method did not differ significantly, but the fewest cells were obtained by PN (Fig 1). Although the fewest cells were obtained from small cell carcinomas, no significant difference was seen according to the histologic type of lung cancer (Fig 2).

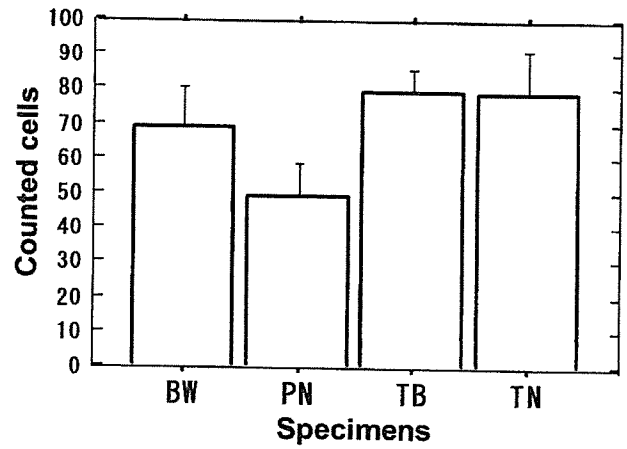

FIGURE 1. Countable cells according to the type of clinical specimen. Although cell counts obtained by PN were the lowest, no statistical significance was obtained by the Kruskal-Wallis test (p = 0.1117). Error bars indicate standard error. TN = transbronchial fine-needle aspiration.

The results of conventional cytology according to the Papanicolau classification were as follows: class I, 4 cases; class II, 15 cases; class IIIa, 3 cases; class IIIb, 5 cases; and class V, 23 cases (Table 2). Twenty-eight cases showing a higher grade than class IIIb were considered to be positive for lung cancer. By cytology, we found no false-positive cases and 11

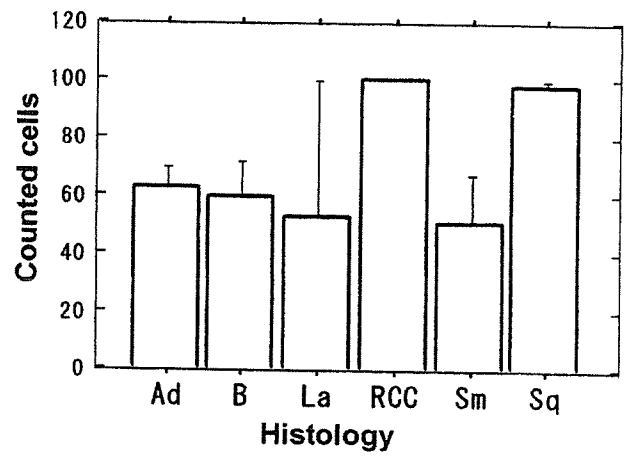

FIGURE 2. Countable cells according to histology. Although cell counts obtained from small cell lung cancer (Sm) were the lowest, no statistical significance was obtained by the Kruskal-Wallis test (p = 0.2369). Error bars indicate SE. Ad = adenocarcinoma; B = benign lesion; La = large cell carcinoma; RCC = renal cell carcinoma; Sq = squamous cell carcinoma.

Table 2—*Results of FISH and Conventional Cytology**

Case	Countable Cells	Three Copies C3/C17	Four Copies C3/C17	Five Copies C3/Ch17	Six Copies or More C3/C17	Hyperdisomy, % C3/C17	FISH	Cytology Stage
1	100	28/18	10/2	2/2	0/0	40/22	Positive	V
2	8	0/0	0/0	0/0	0/0	0/0	Negative	II
3	100	14/9	4/4	1/1	0/0	18/13	Positive	V
4	100	16/8	0/1	1/0	0/0	17/9	Positive	II†
5	52	2/0	1/0	0/0	0/0	3/0	Negative†	II†
6	100	9/0	1/3	1/0	0/0	10/3	Positive	IIIa†
7	44	7/3	0/0	1/0	0/0	18/7	Positive	II†
8	100	6/6	0/2	2/2	0/0	8/10	Positive	V
9	5	0/0	0/0	0/0	0/0	0/0	Negative†	I†
10	100	17/26	2/5	1/2	0/0	20/33	Positive	II†
11	100	38/37	9/2	3/0	1/0	51/39	Positive	V
12	17	2/3	2/1	1/0	0/0	29/29	Positive	V
13	79	5/11	5/3	4/1	0/0	18/19	Positive	IIIb
14	100	7/3	0/0	0/0	1/0	8/3	Negative†	II†
15	100	9/0	1/3	1/0	0/0	11/3	Positive	II†
16	42	0/1	0/0	0/0	0/0	0/2	Negative	II
17	100	22/16	2/11	3/5	0/1	27/33	Positive	V
18	100	2/0	0/0	0/0	0/0	2/0	Negative	I
19	26	5/8	0/0	0/0	0/0	19/31	Positive	IIIb
20	100	1/1	0/0	0/0	0/0	1/1	Negative	II
21	100	0/0	0/0	0/0	0/0	0/0	Negative	II
22	100	17/14	3/1	2/2	1/1	23/18	Positive	IIIb
23	5	1/1	0/0	0/0	0/0	20/20	Positive	IIIb
24	100	22/23	5/7	1/3	2/1	30/34	Positive	V
25	37	13/10	1/7	1/0	0/0	41/46	Positive	V
26	8	0/0	0/0	0/0	0/0	0/0	Negative	IIIa
27	43	1/1	0/0	0/0	0/0	2/2	Negative†	I†
28	100	0/0	0/0	0/0	0/0	0/0	Negative	I
29	44	0/0	0/1	0/0	0/0	0/2	Negative	II
30	100	8/6	1/1	0/1	0/0	9/8	Negative†	IIIb
31	100	2/0	0/0	0/0	0/0	2/0	Negative	II
32	8	2/3	1/1	1/0	0/0	50/50	Positive	V
33	21	4/5	1/0	0/0	0/0	24/24	Positive	V
34	57	27/31	5/2	2/1	0/1	60/61	Positive	V
35	40	10/9	2/3	4/0	0/2	40/35	Positive	V
36	100	15/15	1/4	1/1	0/0	17/20	Positive	V
37	38	2/4	0/0	0/0	0/0	5/11	Positive	V
38	23	0/1	0/0	0/0	0/0	0/4	Negative	II
39	45	9/9	1/4	2/1	0/0	27/31	Positive	V
40	79	14/12	1/1	1/0	0/0	20/16	Positive	V
41	30	0/1	0/0	0/0	0/0	0/3	Negative	II
42	100	17/6	3/1	0/1	0/0	20/8	Positive	V
43	100	19/18	3/6	4/1	2/0	28/25	Positive	II†
44	100	18/15	1/5	0/1	0/0	19/21	Positive	V
45	100	11/7	0/1	0/0	0/0	11/8	Positive	V
46	14	4/3	0/0	0/0	0/0	29/21	Positive	V
47	100	15/15	0/8	0/1	0/0	15/24	Positive	V
48	48	8/6	0/1	0/0	0/0	17/15	Positive	V
49	25	4/6	1/0	0/0	0/0	20/24	Positive	V
50	100	21/28	5/5	1/1	0/0	27/34	Positive	IIIa†

*C3 = chromosome 3; C17 = chromosome 17.
†False-negative result.

false-negative cases. Thus, by conventional cytology, specificity was 100%, and sensitivity was 71.8%.

In FISH analyses, 34 cases showed aberrant copy numbers in either chromosome 3 or 17. Representative findings of conventional cytology and FISH are shown in Figure 3. We found no false-positive cases and five false-negative cases. For FISH analyses, specificity was 100%, and sensitivity was 87.1%.

Seven cases, including one with metastatic renal cell carcinoma, had negative cytology findings and

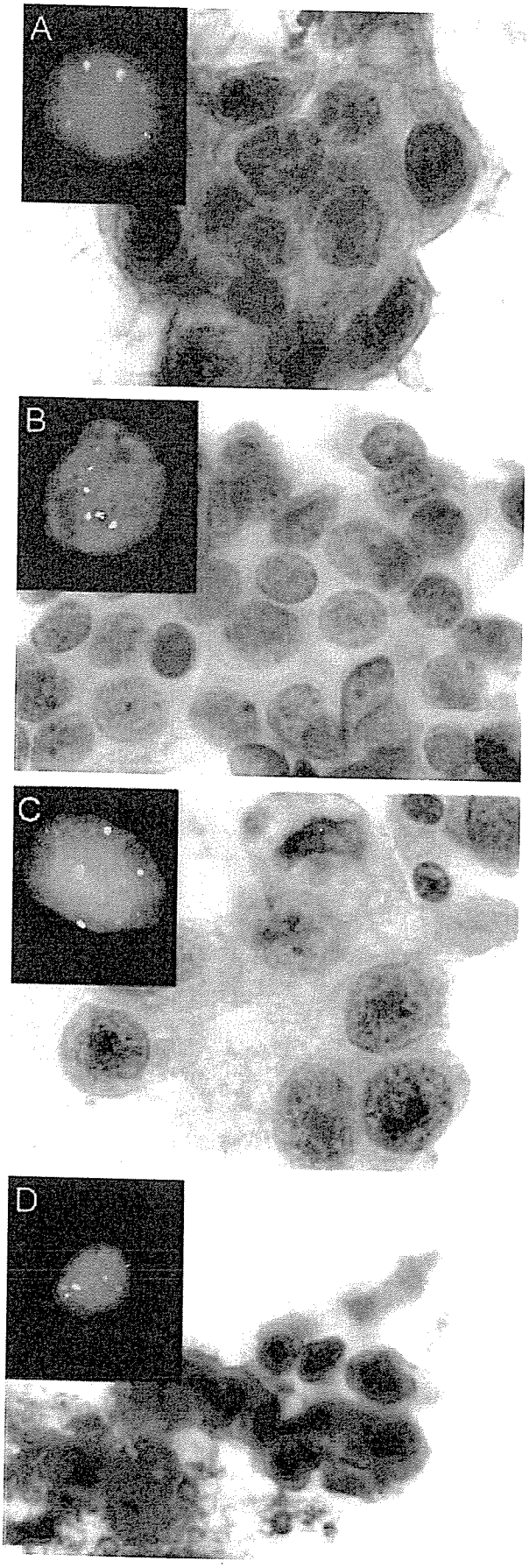

positive FISH findings. In these cases, the cytologic classifications were as follows: class II, five cases; and class IIIa, two cases. One case was cytology-positive and FISH-negative. In this case, the portion of aneusomic cells were observed to be 8 to 9%, which is just below the predetermined cutoff value.

Discussion

We demonstrated here the usefulness of FISH analyses in diagnosing lung cancer using various clinical specimens. Similar results about the effectiveness of FISH analyses have been reported by several authors. Schenk et al[20] examined 23 patients with lung cancer by FISH with probes specific for chromosomes 3, 8, 11, 12, 17, and 18 for malignant effusions and primary tumors. In that study, chromosomal alterations always consisted of gains in chromosomal signal numbers, and all chromosomes were found to be aneusomic to a similar extent. According to this observation, we used only two probes in the present study, which were specific for chromosomes 3 and 17.

Recently, Sokolova et al[21] analyzed BW specimens from 48 patients with lung cancer by FISH using four probes (*ie*, centromeric region of chromosome 1, 5p15, 8q24 (c-myc), and 7p12 [epidermal growth factor receptor]). In that report, FISH detected 15 of 18 specimens that were falsely negative by cytology. The sensitivity of FISH for the detection of lung cancer was 82% compared with 54% sensitivity by conventional cytology. The same group[22] used a similar FISH probe set to show that significantly higher frequencies of abnormal cells were found in each of the 20 surgical specimens of non-small cell carcinoma (100%) and in the 3 sputum specimens (100%) from lung cancer patients. These probes detected a 4.8 to 7.3% rate of abnormal copy numbers in normal control specimens. In these retrospective studies, FISH detected lung cancer cells in touch preparations of resected tumors and BWs. Thus, we planned a prospective study to compare conventional cytology with FISH using various specimens from lung lesions.

In our study, we determined the cutoff value for the percentage ofhyperdisomic cells to be 10%, be-

FIGURE 3. Hyperdisomic cells detected by FISH. Red signals are the centromeric region of chromosome 3, and green signals are the centromeric region of chromosome 17.Representative findings of conventional cytology (Papanicolaou stain, original ×400) and FISH in the same cases, as follows: *top left*, *A*: adenocarcinoma (case 39); *top right*, *B*: squamous cell carcinoma (case 1); *bottom left*, *C*: large cell carcinoma (case 24); and *bottom right*, *D*: small cell carcinoma (case 11).

cause we often count ≦6% hyperdisomic cells in normal cell specimens, probably due to counting sister chromatids as two copies. When we set the cutoff value at 10%, a specificity of 100% and a sensitivity of 87.1% were obtained by FISH, whereas the sensitivity of cytology was 71.8%. As a result, we successfully detected seven lung cancer cases that were cytology-negative. Among these cases, two were class IIIa that we could not diagnose as malignant based on morphologic features. FISH may provide decisive information for the detection of malignancies, especially cases with IIIa classification.

Although the sensitivity of FISH is superior to that of conventional cytology, there are some disadvantages to FISH analyses. First, we do not generate information about the histologic type of lung cancer since we cannot observe morphologic features. Second, FISH is expensive. Third, FISH signal counting under fluorescence microscopy is time-consuming. Thus, the present FISH assay system probably can play a complementary role to that of conventional cytology.

We had five cases that we could not correctly diagnose by FISH. There are two possible reasons for our false-negative FISH results. One would be the failure to obtain proper cell material from the lesion, resulting in the absence of cancer cells on the slide. The other would be that the cancer cells were near-diploid, such that we could not detect aneusomy in two target chromosomes. We could probably detect more aneusomic cells using additional suitable probes for other chromosomes or chromosomal regions as reported by Romeo et al,[22] who successfully diagnosed 100% of lung cancer cases by FISH using a set of four probes. In our previous study,[23] chromosomal instability detected by FISH was associated with poor survival in patients with lung cancer. The finding of multiple chromosomal changes by FISH may be used as a prognostic factor and in the selection of patients for different therapeutic programs in the future.

In conclusion, FISH can detect lung cancer cells with aneusomy in various clinical specimens. The sensitivity was superior to that of conventional cytology. FISH should be used in conjunction with conventional cytology.

References

1 Muers M, Boddington M, Cole M, et al. Cytological sampling at fibreoptic bronchoscopy: comparison of catheter aspirates and brush biopsies. Thorax 1982; 37:457–461

2 Schenk D, Bryan C, Bower J, et al. Transbronchial needle aspiration in the diagnosis of bronchogenic carcinoma. Chest 1987; 92:83–85

3 Saji H, Nakamura H, Tsuchida T, et al. The incidence and the risk of pneumothorax and chest tube placement after percutaneous CT-guided lung biopsy: the angle of the needle trajectory is a novel predictor. Chest 2002; 121:1521–1526

4 Ng A, Horak G. Factors significant in the diagnostic accuracy of lung cytology in bronchial washing and sputum samples: I. Bronchial washings. Acta Cytol 1983; 27:391–396

5 Papanicolaou G. Criteria of malignancy. In: Atlas of exfoliative cytology. Cambridge, MA: Harvard University Press, 1954; 13–21

6 Choma D, Daures J-P, Quantin X, et al. Aneuploidy and prognosis of non-small-cell lung cancer: a meta-analysis of published data. Br J Cancer 2001; 85:14–22

7 Nowell P. The clonal evolution of tumor cell populations. Science 1976; 194:23–28

8 Hoglund M, Gisselsson D, Sall T, et al. Coping with complexity. Multivariate analysis of tumor karyotypes. Cancer Genet Cytogenet 2002; 135:103–109

9 Lengauer C, Kinzler K, Vogelstein B. Genetic instabilities in human cancers. Nature 1998; 396:643–649

10 Duesberg P, Rausch C, Rasnick D, et al. Genetic instability of cancer cells is proportional to their degree of aneuploidy. Proc Natl Acad Sci U S A 1998; 95:13692–13697

11 Cahill D, Lengauer C, Yu J, et al. Mutations of mitotic checkpoint genes in human cancers. Nature 1998; 392:300–303

12 Pihan G, Doxsey S. The mitotic machinery as a source of genetic instability in cancer. Semin Cancer Biol 1999; 9:289–302

13 Pinkel D, Straume T, Gray J. Cytogenetic analysis using quantitative, high-sensitivity, fluorescence hybridization. Proc Natl Acad Sci U S A 1986; 83:2934–2938

14 Gingrich J, Shadravan F, Lowry S. A fluorescence *in situ* hybridization map of human chromosome 21 consisting of 30 genetic and physical markers on the chromosome: localization of 137 additional YAC and cosmid clones with respect to this map. Genomics 1993; 17:98–105

15 Kuo W, Tenjin H, Segraves R, et al. Detection of aneuploidy involving chromosomes 13, 18, or 21, by fluorescence *in situ* hybridization (FISH) to interphase and metaphase amniocytes. Am J Hum Genet 1991; 49:112–119

16 Kallioniemi O, Kallioniemi A, Kurisu W, et al. ERBB2 amplification in breast cancer analyzed by fluorescence *in situ* hybridization. Proc Natl Acad Sci U S A 1992; 89:5321–5325

17 Gray J, Collins C, Henderson I, et al. Molecular cytogenetics of human breast cancer. Cold Spring Harb Symp Quant Biol 1994; 59:645–652

18 Hiraguri S, Godfrey T, Nakamura H, et al. Mechanisms of inactivation of E-cadherin in breast cancer cell lines. Cancer Res 1998; 58:1972–1977

19 Mountain C. Revisions in the International System for Staging Lung Cancer. Chest 1997; 111:1710–1717

20 Schenk T, Ackermann J, Brunner C, et al. Detection of chromosomal aneuploidy by interphase fluorescence *in situ* hybridization in bronchoscopically gained cells from lung cancer patients. Chest 1997; 111:1691–1696

21 Sokolova I, Bubendorf L, O'Hare A et al. A fluorescence *in situ* hybridization-based assay for improved detection of lung cancer cells in bronchial washing specimens. Cancer 2002; 96:306–315

22 Romeo M, Sokolova I, Morrison L, et al. Chromosomal abnormalities in non-small cell lung carcinomas and in bronchial epithelia of high-risk smokers detected by multi-target interphase fluorescence *in situ* hybridization. J Mol Diagn 2003; 5:103–112

23 Nakamura H, Saji H, Idiris A, et al. Chromosomal instability detected by fluorescence *in situ* hybridization in surgical specimens of non-small cell lung cancer is associated with poor survival. Clin Cancer Res 2003; 9:2294–2299

Systemic Antitumor Effect of Intratumoral Injection of Dendritic Cells in Combination with Local Photodynamic Therapy

Hisashi Saji,[1,3] Wenru Song,[2] Katsuyoshi Furumoto,[1] Harubumi Kato,[3] and Edgar G. Engleman[1]

Abstract

Purpose: Photodynamic therapy (PDT), which is used clinically for the palliative treatment of cancer, induces local tumor cell death but has no effect on tumors in untreated sites. The purpose of this study was to determine if local PDT followed by intratumoral injection of naïve dendritic cells (IT-DC) induces systemic antitumor immunity that can inhibit the growth of untreated as well as PDT + IT-DC – treated tumors.

Experimental Design: BALB/c or C57Bl/6 mice were injected s.c. with CT26 colorectal carcinoma cells and B16 melanoma cells, respectively, and following 10 to 12 days of tumor growth, the tumors were treated with PDT alone or PDT followed by IT-DC or IT-PBS. In other studies, tumors were established simultaneously in both lower flanks or in one flank and in the lungs, but only one flank was treated.

Results: Whereas neither PDT nor IT-DC alone was effective, PDT + IT-DC eradicated both CT26 and B16 tumors in a significant proportion of animals and prolonged the survival of mice of which the tumors were not cured. The spleens of mice treated with PDT + IT-DC contained tumor-specific cytotoxic and IFN-γ-secreting T cells whereas the spleens of control groups did not. Moreover, adoptive transfer of splenocytes from successfully treated CT26 tumor-free mice protected naïve animals from a subsequent challenge with CT26, and this was mediated mainly by CD8 T cells. Most importantly, PDT plus IT-DC administered to one tumor site led to tumor regression at distant sites, including multiple lung metastases.

Conclusions: PDT + IT-DC induces potent systemic antitumor immunity in mice and should be evaluated in the treatment of human cancer.

Dendritic cells (DC) are the most potent antigen-presenting cells known, uniquely capable of activating both the cognate and innate arms of the immune system. For example, administration of DCs loaded *ex vivo* with tumor-associated antigens can elicit antitumor immunity resulting in tumor regression in various murine models, and DCs pulsed with tumor derived peptides, proteins, genes or lysates, as well as DCs fused with tumor cells, have all been studied as therapeutic cancer vaccines (1–11). Although the methods are complex and costly to implement, promising results have been obtained in clinical trials in patients with advanced malignancies. These trials have shown DC-based vaccination to be well tolerated and capable of inducing tumor-specific T-cell responses and regression of metastatic disease. On the other hand, the overall therapeutic efficacy of this approach has been limited, indicating a need to either enhance its potency or combine it with other treatment modalities.

Among the modalities that might be combined with DC-based immunotherapy are systemically administered antitumor drugs as well as locally targeted therapies such as radiation, radiofrequency ablation, and photodynamic therapy (PDT). PDT has been approved in the United States and other countries as an anticancer therapy, mainly for the palliative treatment of surgically inaccessible tumors. PDT involves the systemic administration of a photosensitizer that preferentially accumulates in transformed cells, followed by illumination of the tumor with a laser beam (12). In the presence of oxygen, the laser light activates the photosensitizer and initiates a complex photochemical reaction that generates cytotoxic intermediates. Tumor destruction after PDT results from direct cytotoxic effects as well as from the induction of a local inflammatory response (12). Thus, preclinical studies have shown that PDT not only mediates apoptotic and necrotic killing of tumor cells but also alters the tumor microenvironment through the release of proinflammatory cytokines such as tumor necrosis factor α, interleukin (IL)-1 and IL-6 (12, 13).

On the basis of its unique mechanism of tumor destruction, PDT has the potential to create an environment at the tumor site that favors both tumor antigen loading and activation of DCs, key requirements for induction of antitumor immunity (14). Because most tumors lack an abundance of DCs, one way to potentially take advantage of this environment would be to inject a sufficient number of autologous DCs directly into

Authors' Affiliations: Departments of [1]Pathology and [2]Medicine, Stanford University School of Medicine, Palo Alto, California and [3]Department of Surgery, Tokyo Medical University, Tokyo, Japan

Received 9/12/05; revised 1/5/06; accepted 1/19/06.

Grant support: National Heart, Lung, and Blood Institute grant HL57443 (E.G. Engleman) and NIH National Cancer Institute grant K08CA105064 (W. Song).

The costs of publication of this article were defrayed in part by the payment of page charges. This article must therefore be hereby marked *advertisement* in accordance with 18 U.S.C. Section 1734 solely to indicate this fact.

Note: H. Saji and W. Song contributed equally to this work.

Requests for reprints: Edgar G. Engleman, Stanford Blood Center, 3373 Hillview Avenue, Palo Alto, CA 94304-1204. Phone: 650-723-7960; Fax: 650-725-0592; E-mail: edengleman@stanford.edu.

doi:10.1158/1078-0432.CCR-05-1986

PDT-treated tumors. Such a strategy alleviates the need to do *in vitro* loading of DCs with tumor antigens because the inflammatory milieu induces DC activation, which facilitates not only antigen acquisition and processing but also migration of the DCs to draining lymph nodes where they interact with a broad range of potential effector cells. In the current study, we evaluated the effect of combining PDT with intratumoral injection of syngeneic DCs (IT-DC) on two histologically distinct murine tumors, CT26 colon carcinoma and B16 melanoma. The results show that this combined treatment induces strong and durable tumor-specific immunity that results in the destruction not only of targeted tumors but also of tumors at distant sites.

Materials and Methods

Mice. Female BALB/c (H-2^d) and C57Bl/6 (H-2^b) mice, 6 to 8 weeks of age, were purchased from The Jackson Laboratory (Bar Harbor, ME). All mice were housed in the Stanford animal facility in accordance with the NIH guidelines.

Cell lines. The murine CT26 colon carcinoma, B16 melanoma (F10 clone), MAD109 lung carcinoma, and EL-4 lymphoma cell lines used in this study were maintained in complete RPMI 1640 with 10% fetal bovine serum, penicillin G (100 units/mL), streptomycin (100 μg/mL), and L-glutamine (10 mmol/L).

DCs. Bone marrow–derived DCs were generated in the presence of granulocyte macrophage colony-stimulating factor and IL-4 for 7 days as previously described (15). Bone marrow cells were harvested from femurs and tibias, and after RBC lysis, the resulting cell suspension was incubated in complete RPMI 1640 containing recombinant murine granulocyte macrophage colony-stimulating factor (10 ng/mL; PeproTech, Inc., Rocky Hill, NJ) and recombinant murine IL-4 (10 ng/mL; PeproTech). On day 2, nonadherent granulocytes were gently removed and fresh medium with granulocyte macrophage colony-stimulating factor and IL-4 was added. On day 5, loosely adherent cells were dislodged and replated. On day 7 of culture, the unpulsed DCs were collected. The maturational status and percentage of DCs were verified by flow cytometry, and staining of three surface markers (CD11c, CD86, and class II antigen) showed the purity of DCs to be ≥74%.

Photosensitizer and laser unit. ATX-S10 Na(II), a hydrophilic chlorin photosensitizer with an absorption maximum at 670 nm (16), was obtained from Photochemical Co. Ltd. (Okayama, Japan). A diode laser (Hamamatsu Photonics, Hamamatsu, Japan) was used as a light source for exciting ATX-S10 Na(II). The diode laser is a continuous-wave laser operating at 670-nm wavelength.

During the light irradiation, mice were anesthetized with ketamine (125 mg/kg: Vedco, Inc., St. Joseph, MO) and xylazine (25 mg/kg; Phoenix Pharmaceutical, Inc., St. Joseph, MO) and were restrained in a specially designed holder.

Combined PDT and IT-DC therapy of CT26 colon cancer. Preliminary studies with ATX-S10 Na(II) and a diode laser, were carried out on the basis of a published protocol (16) to identify a drug dose and laser setting for inhibition of growth of CT26 tumors *in vivo* without major local or systemic toxicity. CT26 tumor cells (10^6 per mouse) in 100 μL HBSS were injected into the lower right flank of BALB/c mice. On day 12, when the average tumor volume was 153.0 ± 11.5 mm^3, the mice received an i.v. injection of ATX-S10 Na(II) (5 mg/kg body weight), followed 4 to 5 hours later by 150 J/cm^2 laser irradiation of the tumor. DCs (1×10^6 per injection in 50 μL PBS) were injected into the tumor on days 13, 14, 15, and 17. The tumor volume was measured thrice a week using a caliper [tumor volume (mm^3) = (longer diameter) × (shorter diameter)^2 × 0.4]. Animals were sacrificed when the tumor diameter exceeded 20 mm or when there were signs of animal distress. Survival was recorded as the percentage of surviving animals on a given day. Surviving mice had no sign of tumor when experiments were terminated.

Combined PDT and IT-DC therapy of B16 melanoma. For the B16 melanoma tumor model, C57Bl/6 mice were inoculated s.c. with 5×10^5 tumor cells in the lower right flank. On day 10, mice with established tumors (average tumor volume, 80.0 ± 5.4 mm^3) were treated with 150 J/cm^2 laser irradiation to the tumor 4 to 5 hours after an ATX-S10 Na(II) (5 mg/kg body weight) injection and given intratumoral injections of DCs on days 11, 12, 13, and 15 (1×10^6 per injection in 50 μL PBS). The measurement of tumor volume and survival was as above.

ELISPOT assays. ELISPOT assays were done with an ELISpot mouse IFN-γ system (R&D Systems, Inc., Minneapolis, MN) according to the instructions of the manufacturer. Splenocytes were isolated 4 weeks after tumor inoculation. After lysis of RBC, splenocytes were resuspended at a final concentration of 5×10^5/mL and 100 μL of this suspension were then incubated at 37°C for 24 hours in ELISPOT plates coated with anti-IFN-γ with 100 μL medium with or without irradiated (30 Gy) stimulator cells (CT26, MAD109, B16, or EL-4).

Cytotoxicity assays. Cytotoxicity was measured by a standard chromium-51(^{51}Cr) release assay. Splenocytes were harvested 4 weeks after tumor inoculation. After lysis of RBC, splenocytes (1×10^6/mL) were stimulated *in vitro* by irradiated (100 Gy) tumor cells (1×10^5/mL) at 37°C for 5 days in the presence of 10 units/mL IL-2. Following culture, splenocytes were separated from dead cells and debris with Lympholyte-M cell separation media (Cederlane Laboratories, Inc., Hornby, Ontario, Canada). Target cells were labeled with ^{51}Cr (200 μCi/5×10^6 cells) for 1 hour at 37°C, washed, and then incubated in U-bottomed wells with effector cells at various effector-to-target cell ratios at 37°C for 4 hours. Spontaneous release and maximum release were determined by incubating target cells in medium alone or in 1% SDS, respectively. Spontaneous release was always <20% of maximum. Radioactivity was counted in a liquid scintillation counter and the percentage of specific target cell lysis was calculated with the formula $[(E - S) / (T - S)] \times 100$, where E is the average experimental release, S is the average spontaneous release, and T is the average maximal release.

Adoptive transfer of splenocytes. To determine whether lymphocytes induced by PDT + IT-DC could protect naïve animals from a tumor challenge, BALB/c mice were inoculated s.c. with CT26 cells and treated with PDT + IT-DC as before. Four weeks later, the splenocytes were harvested and 1×10^7 cells were infused i.v. into naïve mice. Control groups of mice received splenocytes from CT26 tumor-bearing mice treated with either IT-PBS alone, IT-DC alone, or PDT + IT-PBS. One day later, these mice were s.c. challenged with a lethal number (1×10^6) of CT26 cells and monitored for tumor volume and survival.

To analyze the role of specific T-cell subsets in tumor protection, splenocytes were harvested from inoculated tumor-free mice treated with PDT + IT-DC, and $CD4^+$ or $CD8^+$ T cells were depleted by using CD4 (L3T4) or CD8a (Ly-2) coupled microbeads and magnetic cell sorting (Miltenyi Biotec, Inc., Auburn, CA). Splenocytes, $CD4^+$ T-cell–depleted splenocytes, or $CD8^+$ T-cell–depleted splenocytes (1×10^7) were infused i.v. into groups of five naïve mice. Control mice received splenocytes from naïve mice. One day later, the mice were s.c. challenged with a lethal number (1×10^6) of CT26 cells and monitored for tumor volume and survival. These depletion conditions were validated by flow cytometry analysis using anti-CD4 (L3T4)-FITC and CD8a (Ly-2)-phycoerythrin monoclonal antibodies (PharMingen, San Diego, CA). The percent depletion of $CD4^+$ and $CD8^+$ cells was 97% and 93%, respectively.

Secondary tumor challenge. To determine the persistence of tumor-specific immunity in the mice treated by PDT + IT-DC, at day 60 after first tumor inoculation, mice showing complete regression of CT26 tumors were given a second s.c. tumor challenge (1×10^6 CT26) in the left lower flank (contralateral to the first injection site). These mice, as well as a control group of naïve mice that were inoculated with 1×10^6 CT26 tumor cells, were monitored for tumor size and survival.

Effect of PDT + IT-DC on contralateral tumors. To determine whether PDT + IT-DC treatment of one s.c. tumor affected an

established contralateral s.c. tumor, CT26 cells (1×10^6) were injected s.c. into both lower flanks of BALB/c mice on day 0. On day 12, tumor-bearing mice were either untreated or treated with combined PDT + IT-DC (using the protocol above) into the tumor on the right side but not into the tumor on the left side. The bilateral tumor-bearing mice were followed for tumor volume on both flanks.

Effect of PDT + IT-DC on multiple distant tumors. BALB/c mice were inoculated s.c. with 1×10^6 CT26 tumor cells on day 0. On day 5, these mice were injected i.v. with 1×10^6 CT26 tumor cells. PDT + IT-DC was administered on day 12 (as above) to the s.c. tumor alone. On day 21 after i.v. tumor inoculation, mice were euthanized and lungs were harvested and fixed with Bouin's solution (Sigma-Aldrich, St. Louis, MO).

Statistical analysis. Differences between groups were analyzed using unpaired two-tailed Student's t test. Survival curves were plotted by the Kaplan-Meier method and comparisons among groups in the survival data were calculated by log-rank test.

Results

Effect of combination treatment with PDT and IT-DC on CT26 tumors. To test the hypothesis that local PDT followed by IT-DC can inhibit primary tumor growth, BALB/c mice were injected s.c. with CT26 tumor cells. On day 12, the tumors reached an average diameter of 10.5 mm and could not be cured with PDT alone (data not shown). PDT was done at that time and syngeneic DCs were injected intratumorally 1 day later (day 13) and again on days 14, 15, and 17. Although the tumors grew rapidly following treatment with PBS alone, IT-DC alone, and PDT + IT-PBS, the combination of PDT + IT-DC resulted in significant suppression of tumor growth ($P < 0.05$ versus all other groups; Fig. 1A). Four of the nine (44%) animals treated with PDT + IT-DC became tumor-free and the overall survival of the PDT + IT-DC group was significantly prolonged compared with other groups (log-rank test, $P = 0.0006$; Fig. 1B). To determine if the combination of PDT + IT-DC results in immunologic memory, mice that had been treated with PDT + IT-DC and were tumor-free following an initial tumor inoculation were rechallenged in the opposite flank with a second lethal inoculation of the same tumor. The results show that these mice not only survived but were completely resistant to this second inoculation (Fig. 1C).

Effect of combination treatment with PDT and IT-DC on B16 tumors. In contrast to CT26 tumors, the B16 melanoma is considered poorly immunogenic and highly aggressive. Moreover, PDT for the treatment of melanoma has had only limited benefit (17), which is attributed to the presence in such tumors of a large amount of light-absorbing melanin pigment that prevents penetration of the laser beam into the tumor tissue. Our preliminary studies showed that PDT alone could not induce any suppression of growth of B16 tumors, even against s.c. tumors as small as 3 mm in diameter (data not shown). Surprisingly, PDT in combination with IT-DC resulted in a striking antitumor effect ($P < 0.05$, versus all other groups; Fig. 2A). Four of seven (57%) mice treated with PDT + IT-DC became tumor-free and the overall survival of the PDT + IT-DC group was significantly prolonged compared with other groups (log-rank test, $P = 0.0004$; Fig. 2B). Interestingly, two of four PDT + IT-DC–treated tumor-free mice developed white hair at sites of treatment, and in one of these mice, white hair could be seen at a site (neck) distant from the PDT site at ~40 days after treatment (Fig. 2C).

In vitro *characterization of the antitumor immune response induced by PDT + IT-DC.* A correlation between *in vitro* tumor-specific IFN-γ production by host-derived T cells and systemic antitumor immunity has been shown in other studies (18, 19). Using ELISPOT assays, we evaluated whether treatment of CT26 tumor-bearing mice with PDT + IT-DC could elicit tumor-specific IFN-γ-secreting T cells. As shown in Fig. 3A, splenocytes from mice treated with PDT + IT-DC contained significantly more tumor-specific IFN-γ-secreting cells than splenocytes from other groups ($P < 0.05$, versus other groups). Moreover, this cytokine was not secreted spontaneously or in response to

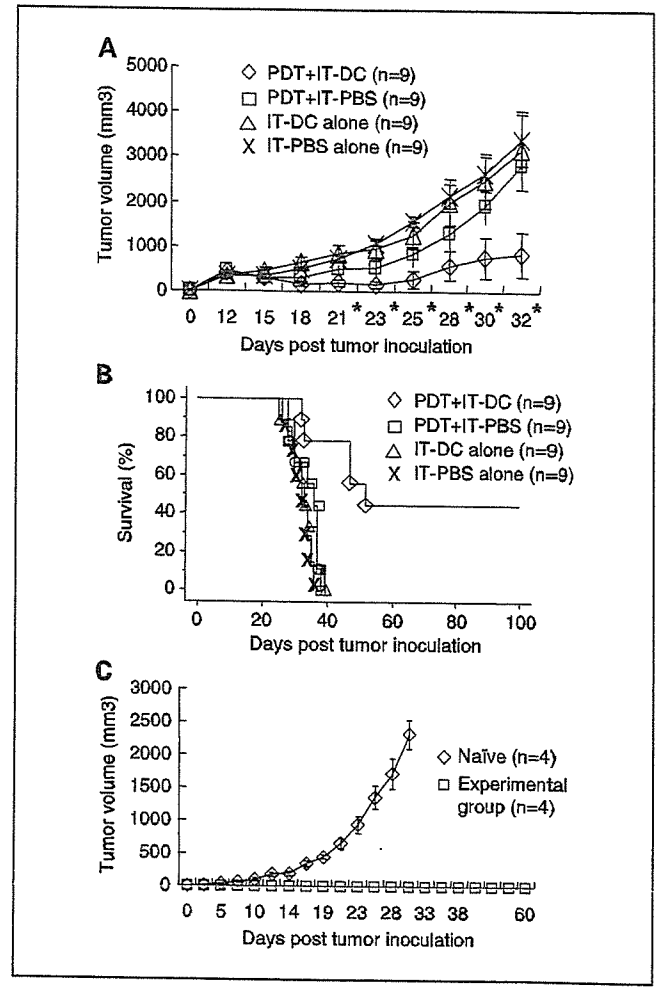

Fig. 1. Effect of combined PDT + IT-DC on the growth of established CT26 syngeneic colon carcinoma tumors. CT26 cells (1×10^6) were injected s.c. in the right lower flank of BALB/c mice. On day 12, mice with established tumors (mean tumor volume 153.0 ± 11.5 mm^3) were treated with PDT as described in Materials and Methods. DCs (1×10^6 in 50 μL PBS) were administered intratumorally on days 13, 14, 15, and 17. The experimental groups included intratumoral injection of PBS alone (50 μL, $n = 9$; ×); intratumoral injection of DCs alone ($n = 9$; △); PDT combined with intratumoral PBS ($n = 9$; □); and PDT combined with IT-DC ($n = 9$; ◇). *A*, mean tumor volume (mm^3) for treatment groups [mean tumor volume = (longer diameter) × (shorter diameter)^2 × 0.4]. Points, mean; bars, SE. *, $P < 0.05$, PDT + IT-DC versus other treatments. *B*, survival of mice recorded as the percentage of surviving animals on a given day. Surviving mice had no sign of tumor when the experiment was terminated. *C*, CT26 tumor rechallenge of tumor-free mice after PDT + IT-DC. Mice that had received CT26 inoculation followed by PDT + IT-DC were rechallenged s.c. with a lethal number (1×10^6) of CT26 tumor cells ($n = 4$; □). Naïve mice inoculated s.c. with the same number of CT26 cells served as controls ($n = 4$; ◇). Experiments were done thrice with similar results.

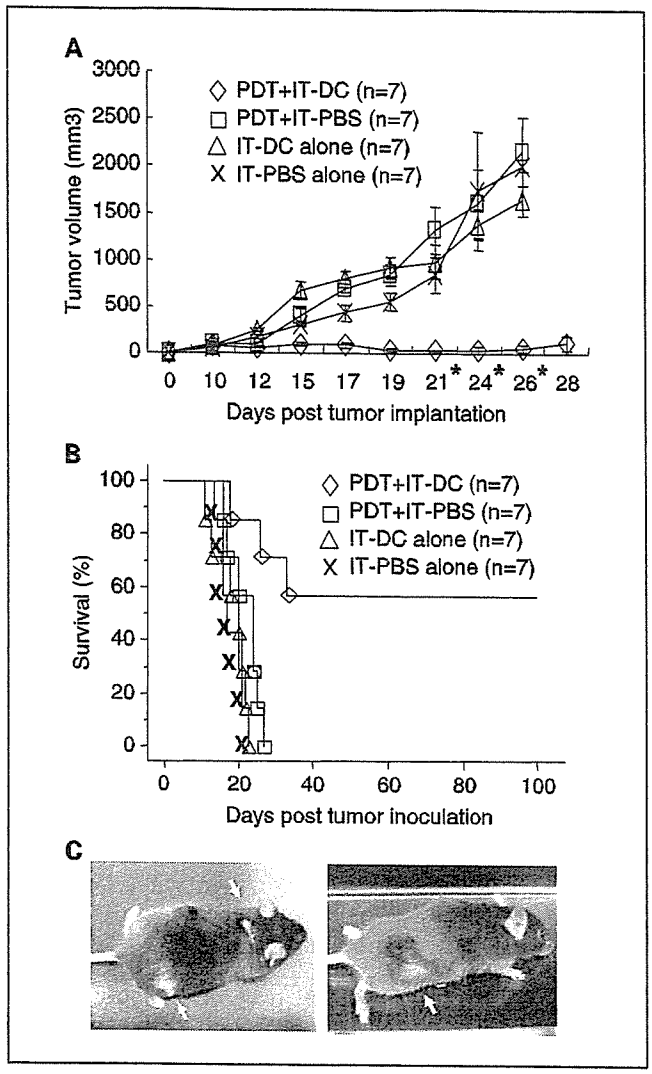

Fig. 2. Effect of PDT + IT-DC on the growth of established B16 melanoma tumors. B16 cells (5×10^5) were injected s.c. in the right lower flank of C57Bl/6 mice. On day 10, mice with established tumors (average tumor size, 80.0 ± 5.4 mm^3) were treated with PDTand received IT-DC (1×10^6 in 50 μL PBS) on days 11, 12, 13, and 15. The experimental groups included IT-PBS alone (50 μL, $n = 7$; ×); IT-DC alone ($n = 7$; △); PDT + IT-PBS ($n = 7$; □); and PDT + IT-DC ($n = 7$; ◇). *A*, mean tumor volume (mm^3) for treatment groups [mean tumor volume = (longer diameter) × (shorter diameter)^2 × 0.4]. Points, mean; bars, SE. *, $P < 0.05$, PDT + IT-DC versus other treatments. *B*, survival of mice recorded as the percentage of surviving animals on a given day. Surviving mice had no sign of tumor when the experiment was terminated. Experiments were done thrice with similar results. *C*, photographs of tumor-free mice taken 60 days after PDT + IT-DC treatment of B16 melanoma. Arrows, white hair growing in an untreated site (neck of mouse on left) and in treated sites (right flanks of both mice).

MAD109 cells, which are irrelevant syngeneic murine lung tumor cells, indicating that the observed response was immunologically specific to CT26 tumor cells. In additional studies, we analyzed the splenocytes of the different treatment groups for the presence of CT26-specific CTLs. Figure 3B shows that such cells were present in the PDT + IT-DC group but not in other groups ($P < 0.05$, versus all other groups). There was no killing of a syngeneic lung cancer cell line (MAD109), indicating that the CTLs are CT26 tumor specific (data not shown).

A tumor-specific immune response was also observed in B16 tumor-bearing mice that had been treated with PDT + IT-DC. As shown in Fig. 4A, splenocytes from such mice contained significantly more tumor-specific IFN-γ-secreting cells compared with splenocytes from control groups ($P < 0.05$). In addition, as shown in Fig. 4B, PDT + IT-DC induced tumor-specific CTLs, as indicated by the presence of such cells in treated but not control animals. No lysis of a syngeneic lymphoma cell line (EL-4) was observed, indicating those CTLs are B16 tumor specific (data not shown).

In vivo *characterization of the antitumor immune response induced by PDT + IT-DC.* To further evaluate the role of CTLs in PDT + IT-DC–induced tumor protection, splenocytes from CT26 inoculated PDT + IT-DC–treated tumor-free mice and splenocytes from control groups were transferred to naïve mice. One day later, the mice were inoculated with a lethal dose of

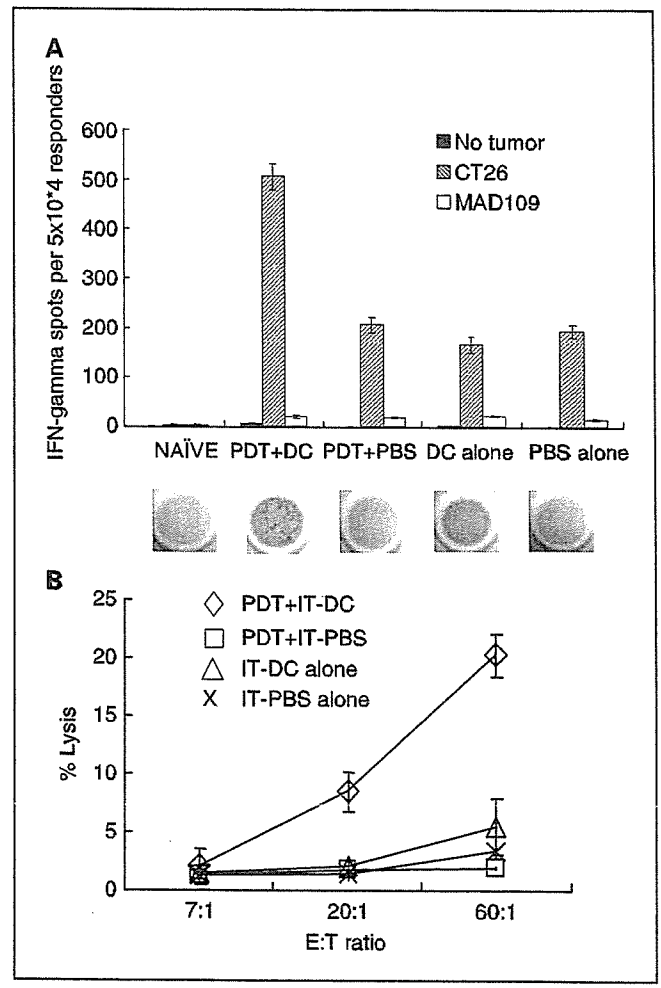

Fig. 3. Induction of *in vitro* anti-CT26 tumor immunity by PDT + IT-DC. *A*, CT26 tumor-bearing mice were treated as detailed in the legend to Fig. 1. Four weeks after tumor inoculation, splenocytes from treated, control, and naïve mice were incubated with or without specific tumor cells or MAD109, irrelevant irradiated tumor cells in an IFN-γ ELISPOTassay. Columns, average number of spots per 5×10^4 responders of triplicate samples; bars, SE. *, $P < 0.05$, versus other groups. Representative ELISPOTwells are shown below the graph. Data are from one of three representative experiments. *B*, CTLs in mice that had been inoculated with CT26 tumor cells followed by treatment with PDT + IT-DC. Four weeks after tumor inoculation, graded numbers of splenocytes from mice receiving various treatment protocols (×, IT-PBS alone; △, IT-DC alone; □, PDT + IT-PBS; ◇, PDT + IT-DC) were cultured in the presence of irradiated CT26 cells for 5 days. Cytotoxicity was measured with a standard 4-hour ^{51}Cr release assay at various ratios of effectors to targets using ^{51}Cr-labeled CT26 cells as targets.

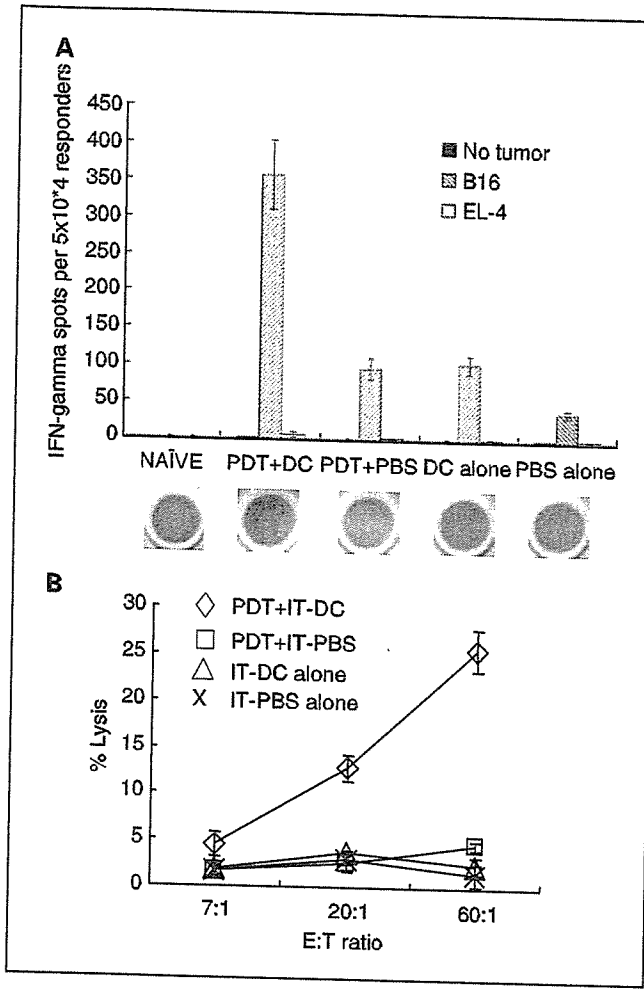

Fig. 4. Induction of anti-B16 tumor immunity by PDT + IT-DC treatment. *A*, B16 tumor–bearing mice were treated as detailed in the legend to Fig. 2. Four weeks after tumor inoculation, splenocytes from treated, control, and naïve mice were incubated with or without specific target cells or irrelevant irradiated tumor cells (EL-4) in an IFN-γ ELISPOTassay. Columns, average number of spots per 5×10^4 responders of triplicate samples; bars, SE. *, $P < 0.05$, versus other groups. Representative wells from an ELISPOT plate are shown below the graph. Data are from one of three representative experiments. *B*, CTLs in mice that received B16 tumor inoculation followed by treatment with PDT + IT-DC. Four weeks after tumor inoculation, graded numbers of splenocytes were cultured in the presence of irradiated B16 tumor cells for 5 days (×, IT-PBS alone; △, IT-DC alone; □, PDT + IT-PBS; ◇, PDT + IT-DC). Cytotoxicity was measured with a 4-hour ^{51}Cr release assay at various ratios of effectors to targets using ^{51}Cr-labeled B16 cells as targets.

CT26 tumor cells. Mice receiving splenocytes from the PDT + IT-DC–treated mice, but not from other mice, were protected from a subsequent tumor challenge with CT26 (Fig. 5A). To determine the role of $CD4^+$ and $CD8^+$ T cells in tumor protection, we repeated this experiment using whole splenocytes or splenocytes depleted of $CD4^+$ or $CD8^+$ T cells. Splenocytes from naïve mice were used as negative controls. One day later, these mice were s.c. challenged with a lethal number of CT26 tumor cells. As shown in Fig. 5B, whereas both $CD4^+$ and $CD8^+$ T cells from PDT + IT-DC–treated mice contributed to tumor protection, CD8 T cells mediated most of the effect.

Effect of PDT + IT-DC on distant untreated tumors. To determine whether treatment of one tumor with PDT + IT-DC conferred systemic antitumor effects, CT26 tumors were established simultaneously in both lower flanks, but only one site was treated with PDT + IT-DC. As shown in Fig. 6A, the growth of both tumors was significantly suppressed compared with the control group, showing that treatment of a primary tumor with PDT + IT-DC confers suppression of the growth of untreated as well as treated tumors. To simulate the clinical scenario in which multiple tumors are present at sites distant from the primary tumor, mice were simultaneously inoculated s.c. in one flank (as above) and i.v. with CT26 tumor cells. This resulted in the seeding of both lungs and the growth of multiple pulmonary metastases. Although a few lesions were visible in the lungs of mice treated with PDT + IT-DC, as shown in Fig. 6B, PDT + IT-DC treatment of the s.c. tumor in such mice resulted in a significant reduction of the lung lesions compared with untreated control animals ($P < 0.05$). Representative examples of lungs from a healthy mouse, a tumor-bearing PDT + IT-DC–treated mouse, and an untreated (control) tumor-bearing mouse are shown in Fig. 6C, D, and E.

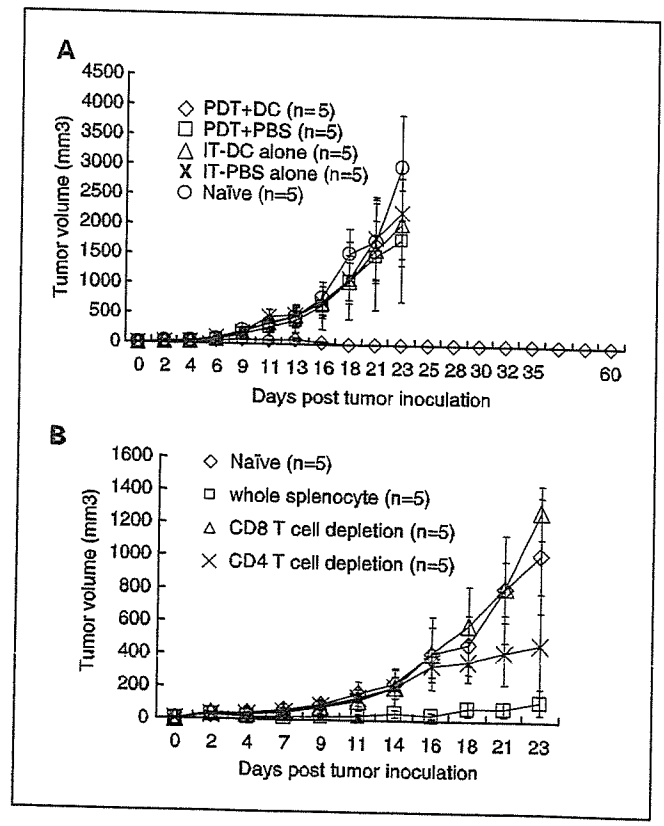

Fig. 5. *A*, adoptive transfer of splenocytes from PDT + IT-DC–treated mice to naïve mice prevents CT26 tumor growth. Splenocytes (1×10^7) from CT26 inoculated mice treated with IT-PBS alone (×), IT-DC alone (△), PDT + IT-PBS (□), or PDT + IT-DC (◇) were infused i.v. into naïve mice. One day later, the mice were challenged s.c. with a lethal number (1×10^6) of CT26 tumor cells. Naïve mice without splenocyte transfer were used as a control (○). Points, average tumor volume (mm^3) of five mice per group; bars, SE. *B*, role of CD4 and CD8 T-cell subsets in protection against CT26 tumors. Splenocytes were harvested from tumor-free mice treated with PDT + IT-DC. $CD4^+$ or $CD8^+$ Tcells in splenocytes were depleted by using CD4 (L3T4) or CD8a (Ly-2) microbead magnetic cell sorting. After magnetic selection, whole splenocytes (□), CD4+ T-cell–depleted splenocytes (×), and CD8+ T-cell–depleted splenocytes (△) were infused i.v. into each of five naïve mice. Mice treated with splenocytes from naïve mice served as a control group (◇). One day later, these mice were s.c. challenged with a lethal number (1×10^6) of CT26 cells and monitored for tumor volume and survival.